Journal of Fluorine Chemistry 144 (2012) 38–44

Contents lists available at SciVerse ScienceDirect

Journal of Fluorine Chemistry

journal homepage: www.elsevier.com/locate/fluor

Hydrogen bonding interactions in two isomers of fluorobenzoylthioureas and their absorption spectra

Wen Yang, Wei Zhu, Weiqun Zhou *, Huanhuan Liu, Jianfen Fan

School of Chemistry, Chemical Engineering and Material Science, Soochow University, 199 Renai Road, Suzhou 215123, People's Republic of China

ARTICLE INFO

Article history:
Received 19 June 2012
Received in revised form 21 August 2012
Accepted 8 September 2012
Available online 1 October 2012

Keywords:
Crystal structure
Intra- and intermolecular hydrogen bonds
UV absorption spectra
DFT method

ABSTRACT

Crystal structures of two benzoylthiourea isomers, named N-4-fluorobenzoyl-N′-4-tolylthiourea (FBTT4) and N-2-fluorobenzoyl-N′-2-tolylthiourea (FBTT2) were determined by X-ray diffraction method. It was found that intra- and intermolecular hydrogen bonds played an essential role in determining their conformations. Electronic spectra of these two isomers (FBTTs) were investigated by UV absorption spectra. The UV absorption bands indicating $n \rightarrow \pi^*$ transition become widened due to intramolecular hydrogen bonds, while intermolecular hydrogen bonds between FBTTs and the solvent molecules led to unusual blue shifts of the UV absorption band for $\pi \rightarrow \pi^*$ transition. The intensity of UV absorption decreased as increasing the solvent polarity and the formation of intermolecular hydrogen bonds. The absorption spectra of two isomers have been calculated with the TDDFT formalism. The calculated absorption curves by the CPCM model considering the first solvent shell match well with the experimental results.

1. Introduction

Intra- and intermolecular hydrogen bonds play a critical role in structure and function of molecules [1–5], and hold the important station in photophysics and photochemistry. For instance, the electronic excited states of the chromophores can be remarkably adjusted by the surrounding intermolecular hydrogen bonds [6–10]. Over the past few years, a variety of anionic fluorescence chemosensors, such as the family of N-substituted N′-carbonyl thiourea compounds, have been successfully developed [11–17]. Of such molecules, benzoylthiourea derivatives show interesting luminescent properties with a very strong impact of the molecular structure on their properties. They have been extensively studied for their applications as 'host' molecules for recognization of 'guest' anions utilizing hydrogen bonds in the field of supramolecular chemistry [18–25]. It has been reported that insertion of fluorine in a strategic position of a molecule has emerged as a very powerful and versatile tool for the development of compounds endowed with biological activities, with changing the steric and electronic parameters [26–33].

DFT method and Beck's three-parameter hybrid method (B3LYP) [34–36] had been employed to optimize the ground structure of FBMPT [37] at the level of 6-31G (d). In the last few years, time-dependent density functional theory (TDDFT) [38–40] has been successfully applied for an accurate description of electronic excitations as well as for predicting absorption and emission spectral characteristics. In the present work the absorption energies for title compounds are calculated using the TDDFT formalism. The solvent effect is modeled using the Polarizable Continuum Model (PCM) [40–43].

FBTT2 has been synthesized by Yavari et al. under solvent-free conditions [44], however, the crystal structures and the electronic spectra of both FBTTs have not been reported. In order to investigate the effects of intra- and intermolecular hydrogen bonds on the photo-physical properties of FBTTs, both FBTT2 and FBTT4 were prepared and structurally and photo-physically characterized. Herein, in combination with quantum chemical calculations, we attempt to explore the effects of hydrogen bonds on the crystal structures and the properties of ultraviolet (UV) absorption of FBTTs, aiming at providing guidance theoretically and experimentally for searching for new fluorescent materials and further exploring their applications in the future.

2. Results and discussion

2.1. Crystal structures

The summary of the experimental X-ray data is presented in Table 1. The structures were solved using SHELXS [45] and refined using the SHELXL program [46]. All hydrogen atom positions were calculated and refined using the riding model. The molecular structures of FBTT2 and FBTT4, the perspective views showing the atomic numbering scheme and the crystal packings are presented in Scheme 1 and Fig. 1. The bond parameters are compiled in Table 2.

* Corresponding author. Tel.: +86 0512 65884827.
E-mail address: wqzhou@suda.edu.cn (W. Zhou).

0022-1139/$ – see front matter © 2012 Elsevier B.V. All rights reserved.
http://dx.doi.org/10.1016/j.jfluchem.2012.09.005

Table 1
Summary of X-ray diffraction data.

Compounds	FBTT4	FBTT2
Crystal system	Monoclinic	Monoclinic
Empirical formula	$C_{15}H_{13}N_2OFS$	$C_{15}H_{13}N_2OFS$
Formula weight	288.33	288.33
Temperature	223(2)	223(2)
Lattice parameters	a = 10.904(2) Å	a = 14.513(6) Å
	b = 6.2780(11) Å	b = 13.445(6) Å
	c = 20.630(4) Å	c = 7.154(3) Å
	β = 94.496(5)°	β = 92.584(11)°
	1407.9(5) Å^3	V = 1394.5(10) Å^3
Space group	$P2_1/n$	$P2_1/c$
Z value	4	4
D_{calc}	1.360 g/cm^3	1.373 g/cm^3
F(000)	600.00	600.00
Radiation (Mo Kα) (Å)	0.71070	0.71070
μ (Mo Kα) (mm^{-1})	0.237	0.240
Crystal dimensions (mm)	0.80 × 0.60 × 0.60	0.60 × 0.30 × 0.20
θ Range (°)	3.39–27.50	3.03–27.62
Reflections collected	8428	7473
Independent reflections	3209	3186
R(int)	0.0248	0.0771
Data	3205	3186
Restraints	0	0
Parameters	184	183
Max. and min. transmission	0.855 and 0.651	0.953 and 0.568
GOF on F^2	1.042	0.86
R_1 [$I > 2\sigma(I)$]	0.0444	0.0630
wR_2 [$I > 2\sigma(I)$]	0.1253	0.1456
R_1 [all data]	0.0580	0.1306
wR_2 [all data]	0.1357	0.1732
Largest difference peak (Å^3)	0.330 and −0.277	0.318 and −0.321

The crystallographic information files are deposited to the Cambridge Crystallographic Data Center as CCDC 836991 for FBTT4 and 836992 for FBTT2. Important intermolecular hydrogen bonding interactions in the crystals are depicted in Table 3.

For FBTT4, one intramolecular hydrogen bond interaction, N(2)–H(2)···O(1) exists with the following parameters: the distance of N(2)···O(1), 2.691 Å, the distance of H(2)···O(1), 2.01 Å, the angle of ∠N(2)–H(2)···O(1), 135°. As for intermolecular hydrogen bonds, one pair is N(1$^{\#}$)–H(1$^{\#}$)···S(1) and N(1)–H(1)···S(1$^{\#}$), with the distance of N(1)···S(1), 3.463 Å, the distance of H(1)···S(1), 2.67 Å, the angle of ∠N(1)–H(1)···S(1), 151.7°. Another pair is N(2$^{\#}$)–H(2$^{\#}$)···O(1) and N(2)–H(2)···O(1$^{\#}$), the distance of N(2)···O(1), 3.186 Å, the distance of H(2)···O(1), 2.48 Å, the angle of ∠N(2)–H(2)···O(1), 139.0°. Other weak intermolecular hydrogen bonds include C(2$^{\#}$)–H(2$^{\#}$)···F(1), symm., (−x+1/2, y−1/2, −z−1/2) and C(2)–H(2)···F(1$^{\#}$), symm., (1/2−x, y+1/2, −1/2−z), in which, the distance of C(2)···F(1) is 3.214 Å, the distance of H(2)···F(1) is 2.47 Å and the angle of ∠C(2)–H(2)···F(1) is 136.3°.

For the molecular structure of FBTT2, two intramolecular hydrogen bonds are observed. N(1)–H(1)···F(1) bears distances of 2.738 Å between N(1) and F(1) and 2.14 Å between H(1) and F(1), with an angle of 125.8° for ∠N(1)–H(1)···F(1). Another hydrogen bond exists in the formation of N(2)–H(2)···O(1), with a distance of 2.696 Å between N(2) and O(1), a distance of 2.02 Å between H(2) and O(1) and an angle of 134° for ∠N(2)–H(2)···O(1). The intermolecular hydrogen bonds are C(4)–H(4)···F(1$^{\#}$), symm., (−x, −1/2−y, 3/2−z) and C(4$^{\#}$)–H(4$^{\#}$)···F(1), symm., (−x, 1/2−y, 3/2−z). The distance of C(4) and F(1) is 3.131 Å, the distance between H(4) and F(1) is 2.49 Å, and the angle of ∠C(4)–H(4)···F(1$^{\#}$) is 125.3°.

The intramolecular hydrogen bonds result in the special molecular configurations and the intermolecular interaction mode, which, in turn, leads to different crystal packing mode. Both molecules are composed of three parts from left to right: benzoyl ring, carbonylthiourea ring composed by the intramolecular hydrogen bond N(2)–H(2)···O(1), and toluidine plane. Due to the steric effect of o-methyl, the difference of the dihedral angles of the carbonylthiourea plane and the toluidine plane in both FBTT molecules is obvious, 60° for FBTT4 and 75.8° for FBTT2,

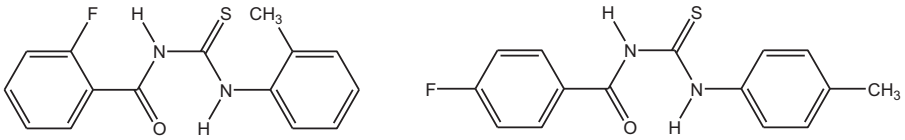

Scheme 1. The molecular structures of FBTT2 and FBTT4.

Table 2
Some structure parameters by X-ray diffraction and MP2 methods.

	FBTT4		FBTT2			FBTT4		FBTT2	
	X-ray	MP2	X-ray	MP2		X-ray	MP2	X-ray	MP2
Bond lengths (Å)					Bond angles (°)				
S(1)–C(8)	1.6658(18)	1.655	1.649(3)	1.654	N(1)–C(7)–C(6)	114.60(13)	114.6	117.2(3)	116.7
O(1)–C(7)	1.226(19)	1.240	1.233(3)	1.241	O(1)–C(7)–C(6)	122.72(15)	121.6	119.9(3)	119.8
N(1)–C(7)	1.373(2)	1.378	1.357(4)	1.372	C(14)–C(9)–N(2)	121.04(14)	123.2	120.7(3)	120.0
N(1)–C(8)	1.394(2)	1.415	1.406(4	1.412	C(10)–C(9)–N(2)	118.94(16)	116.7	117.8(3)	118.2
N(2)–C(8)	1.333(2)	1.348	1.341(4)	1.347	F(1)–C(3)–C(2) F(1)–C(1)–C(2)	118.40(17)	118.8	118.1(3)	116.6
N(2)–C(9)	1.433(2)	1.414	1.440(4)	1.427	F(1)–C(3)–C(4) F(1)–C(1)–C(6)	118.35(18)	118.8	119.4(3)	120.6
F(1)–C(3) F(1)–C(1)	1.357(19)	1.354	1.352(4)	1.368					
Bond angles (°)					Torsion angles (°)				
C(7)–N(1)–C(8)	129.32(13)	130.1	130.1(3)	129.0	C(5)–C(6)–C(7)–O(1)	−29.3(2)	−28.9	27.7(5)	7.0
C(8)–N(2)–C(9)	124.32(14)	128.4	122.3(3)	123.3	C(1)–C(6)–C(7)–O(1)	148.70(17)	151.1	−149.4(3)	−171.9
N(2)–C(8)–N(1)	116.40(14)	113.1	115.3(3)	114.7	C(5)–C(6)–C(7)–N(1)	150.65(15)	150.2	−152.4(3)	−171.7
N(2)–C(8)–S(1)	125.24(13)	129.1	126.3(2)	126.7	C(1)–C(6)–C(7)–N(1)	−31.3(2)	−30.6	30.5(5)	9.3
N(1)–C(8)–S(1)	118.36(11)	129.1	118.4(2)	118.6	C(8)–N(2)–C(9)–C(14)	60.0(2)	39.1	−75.8(4)	−80.2
O(1)–C(7)–N(1)	122.68(15)	123.8	123.0(3)	123.5	C(8)–N(2)–C(9)–C(10)	−122.43(18)	−145.5	106.1(4)	104.0

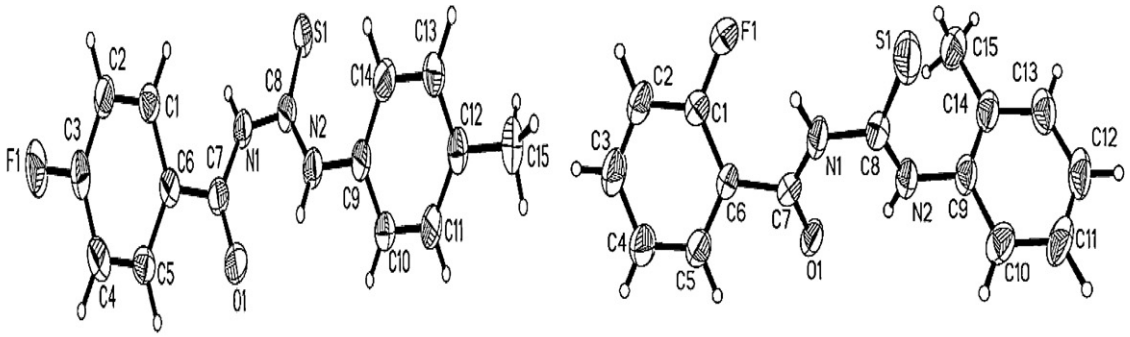

The structures by X-ray; ellipsoids were plotted at the 40% probability

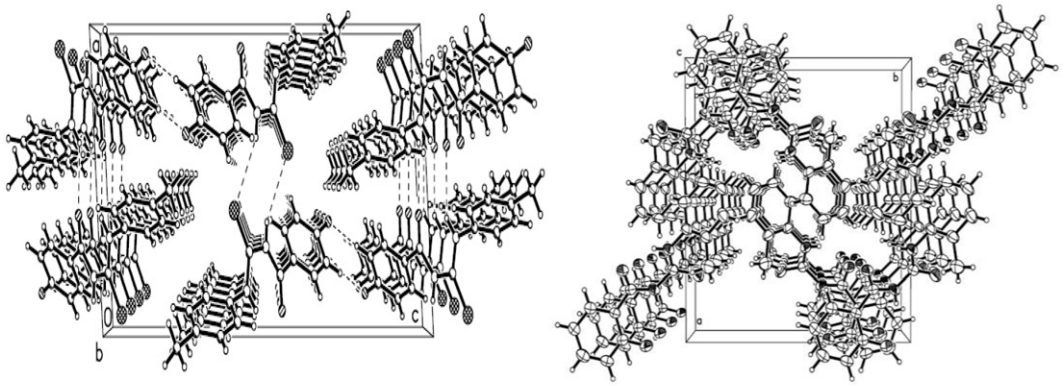

The crystal of packing along axis c

The crystal of packing along axis b

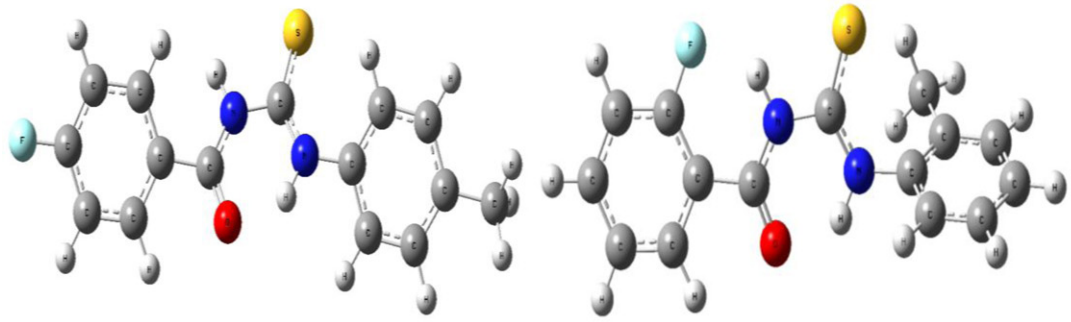

Optimized molecular structures obtained by MP2 method

FBTT4 FBTT2

Fig. 1. Crystal structures with thermal ellipsoids drawn at 40% probability, the crystal of packing and optimized molecular structures obtained by MP2 method of FBTT4 and FBTT2.

respectively. Little difference is found in bond lengths and bond angles for the two crystal molecules.

As discussed above, intramolecular hydrogen bonds affect the hydrogen bond interactions between molecules. On the other hand, intermolecular hydrogen bond interactions also affect molecular structures and the intramolecular hydrogen bond interactions. The optimized molecular structures of both FBTTs by MP2/6-31G (d) are also shown in Fig. 1. If we consider the optimized structure by MP2 method as the criterion for FBTT4, because of the two intermolecular hydrogen bonds N($2^{\#}$)–H($2^{\#}$)···O(1) and N(2)–H(2)···O($1^{\#}$), the dihedral angle, D(C(8)–N(2)–C(9)–C(14)), increases from 39.1° obtained by MP2 method to 60° in the molecule of the crystal. For FBTT2, the intermolecular hydrogen bonds, C(4)–H(4)...F($1^{\#}$) and C($4^{\#}$)–H($4^{\#}$)...F(1) weaken the intramolecular hydrogen bond, N(1)–H(1)...F(1). The dihedral angle D(C(1)–C(6)–C(7)–N(1)), 30.5° in the crystal structure is larger than 9.3°, calculated by MP2 method.

2.2. UV Spectra

The UV visible spectra are shown in Fig. 2, with the maximum absorption wavelengths of FBTTs listed in Table 4. Generally, a B band of $\pi \rightarrow \pi^*$ transition exhibits a red shift and an R band of $n \rightarrow \pi^*$ transition exhibits a blue shift as the polarity of the solvent increases [47]. For FBTT4, the maximum wavelength, λ_{a1}, of the first absorption band at 315 nm in cyclohexane shifts blue to

Table 3
Intra- and intermolecular hydrogen bonds in FBTTs (distance: Å, angle:°).

FBTT4			FBTT2		
Intramolecular	Distances		**Intramolecular**	Distances	FBTT4
N(2)–H(2)···O(1)	N(2)···O(1)	2.691(2)	N(1)–H(1)···F(1)	N(1)···F(1)	2.738(3)
	H(2)···O(1)	2.01		H(1)···F(1)	2.14
	∠N(2)–H(2)···O(1)	135.0		∠N(1)–H(1)···F(1)	125.8
Intermolecular			N(2)–H(2)···O(1)	N(2)···O(1)	2.696(3)
N(1)–H(1)···S(1$^{\#}$)	N(1)···S(1)	3.4635(14)		H(2)···O(1)	2.02
N(1$^{\#}$)–H(1$^{\#}$)···S(1)	H(1)···S(1)	2.67		∠N(2)–H(2)···O(1)	134.0
Symm. op. (−*x*,1−*y*, −*z*)	∠N(1)–H(1)···S(1)	151.7			
N(2$^{\#}$)–H(2$^{\#}$)···O(1)	N(2)···O(1)	3.1862(19)	**Intermolecular**		
N(2)–H(2)···O(1$^{\#}$)	H(2)···O(1)	2.48	C(4)–H(4)···F(1$^{\#}$)	C(4)···F(1)	3.131(4)
Symm. op. (1−*x*, 1−*y*, −*z*)	∠N(1)–H(1)···O(1)	139.0	Symm. op. (−*x*, −1/2−*y*, 3/2−*z*)	H(4)···F(1)	2.49
			C(4$^{\#}$)–H(4$^{\#}$)···F(1)	∠C(4)–H(4)···F(1)	125.3
C(2)–H(2)···F(1$^{\#}$)	C(2)···F(1)	3.214	Symm. op. (−*x*, 1/2−*y*, 3/2−*z*)		
Symm. op. (1/2−*x*, 1/2+*y*, −1/2−*z*)	H(2)···F(1)	2.47	C(4)–H(4)···F(1$^{\#}$)		
C(2$^{\#}$)–H(2$^{\#}$)···F(1)	∠C(2)–H(2)···F(1)	136.3			
Symm. op. (1/2−*x*, −1/2+*y*, −1/2−*z*)					

312 nm in THF, 306 nm in dichloromethane and 290 nm in acetonitrile and methanol with the increase of the polarity of the solvent, which shows n → π* nature. The maximum wavelength of the second absorption band, λ_{a2}, at 264 nm in cyclohexane bathochromic shifts to 280 nm in dichloromethane and 295 nm in THF as the increase of the solvent polarities, indicating its π → π* nature. The solvent effect of the shift results from the stabilization of the excited states by increasing solvent polarity, that is to say, the molecular structure of excited state is more polar than that of ground state. The absorption intensity of the second band dramatically decreases so that it is covered by the absorption band (λ_{a1}) in THF. The uncommon blue shift of the second absorption band presents with the increase of the polarity of the solvent further. Both maximum absorption wavelengths, λ_{a2}, appear at about 265 nm in acetonitrile and methanol. The phenomenon is related to the existence of the intermolecular hydrogen bonds between the FBTT4 and solvent molecules. The intensity of both absorption bands decreases as the polarity of the solvent increases.

The UV absorption curves of FBTT2 in five solvents are similar to those of FBTT4. The first absorption wavelength, λ_{a1}, of n → π* nature is at 318 nm in cyclohexane. The first blue shift absorption

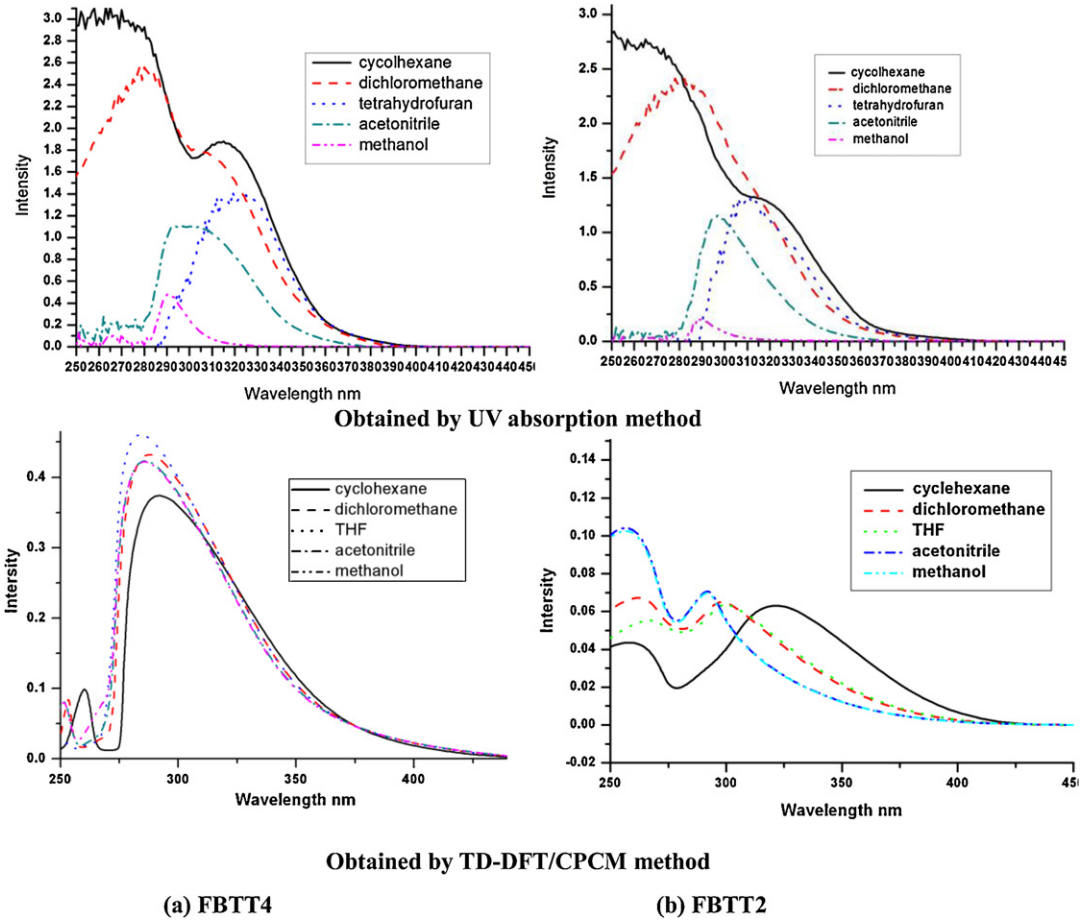

Fig. 2. Absorption curves of experiments and calculations for both FBTTs in the studied solvents.

Table 4
The maxima absorption wavelengths by UV and TD-DFT calculations.

Compounds	Solvents	λ_{a2} (nm)		λ_{a1} (nm)	
		Experimental	TD/CPCM	Experimental	TD/CPCM
FBTT4	Cyclohexane	264	265	315	292
	Dichloromethane	280	253	306	291
	THF	295	253	312	291
	Acetonitrile	265	252	290	289
	Methanol	265	252	290	289
FBTT2	Cyclohexane	264	258	318	325
	Dichloromethane	285	262	298	
	THF	309	264	306	
	Acetonitrile	273	255	292	290
	Methanol	273	255	290	290

band with the polarity of the solvent increasing is covered by the second band, the bathochromic shift band of $\pi \rightarrow \pi^*$ nature in dichloromethane and THF. Comparing with the UV absorption spectra of FBTT4, the existence of the intramolecular hydrogen bond, N–H···F in FBTT2 broadens the first absorption band. The widening of the absorption band results in the appearance of only a shoulder peak in cyclohexane. The absorption peaks have been covered by the second absorption bands in THF and dichloromethane, therefore it cannot be detected. The maximum wavelength, of the second absorption band (λ_{a2}) is at about 264 nm in cyclohexane. It shifts red to 285 nm in dichloromethane and 309 nm in THF and shifts blue to 273 nm in acetonitrile and methanol. The intensity of both absorption bands decreases as the polarity of the solvent increases. The intensity of these bands in acetonitrile and methanol is too weak to be detected.

The intermolecular hydrogen bond interactions between FBTTs and solvent molecules result in the uncommon blue shifts in acetonitrile and methanol. Limited in the computer resources, we consider the molecular complexes of the short-range intermolecular hydrogen bond interactions of the first solvent-shell as solvent effect. Taking FBTT4 as an example, the optimized complexes by MP2 method of FBTT4 with the solvents, methanol and acetonitrile are displayed in Fig. 3. In the complexes, the methanol molecules act as the donor as well as the acceptor in the hydrogen bond interaction. One acetonitrile molecule only acts as the donor and the other as the donor as well as the acceptor in the hydrogen bond interaction.

Frontier molecular orbitals (FMOs) are shown in Fig. 4. Both FBTTs have similar FMOs. Lowest unoccupied molecular orbitals (LUMO) are situated at the part of benzoylthiourea, which is a π conjugated orbital. The highest occupied molecular orbital (HOMO) locates partly on aniline, thiocarbonyl and methyl. Thus, the HOMO involves the lone pairs of sulfur. However, the lone pairs of electrons of sulfur, which is twisted out of the plane of the aromatic ring, cannot conjugate with the aromatic ring. The first transition, HOMO → LUMO, possesses the property of $n \rightarrow \pi^*$ transition. Hence, the blue shift in polar solvent can be observed. The next highest occupied molecular orbital (HOMO-1) is a π conjugated orbital including the part of anilinethiourea. Therefore, the second transition, HOMO-1 → LUMO, must be the transition of $\pi \rightarrow \pi^*$, and the red shift in polar solvents can be observed.

Solvent effects are calculated by CPCM model in cyclohexane, dichloromethane and THF. In acetonitrile and methanol, because of the existence of the intermolecular hydrogen bond interactions between the FBTTs and the solvent molecules, the CPCM model is used on the molecular complexes with the solvent molecules. The simulated UV–visible absorptions are also shown in Fig. 2. The calculated maximum absorption wavelengths are compiled in Table 4. For FBTT4, in solution with a concentration of 10^{-4} mol L^{-1}, the number of solvent molecules are more than solute molecules. The calculated model added a micro-solvent shell considers the intermolecular interactions between FBTT4 and solvent molecules and omits the interactions between FBTT4 molecules. Thus, the calculation should be effective. The calculated absorption curves of FBTT4 in acetonitrile and methanol are similar to that observed in experimental UV visible spectra. For example, in methanol, the wavelength of the second absorption band obtained from calculation is 253 nm and the corresponding value in experiment is 265 nm, with an error of only 12 nm. The difference between the calculations and the experiments is found in cyclohexane, dichloromethane and THF. The calculated second absorption bands shift blue slightly, whereas the absorption bands of the UV spectra shift red. The difference may result from the overlook of the interaction between the solute molecules. The CPCM model only considers the solvent molecules as dipoles. However, hydrogen bond interactions are larger than usual dipole

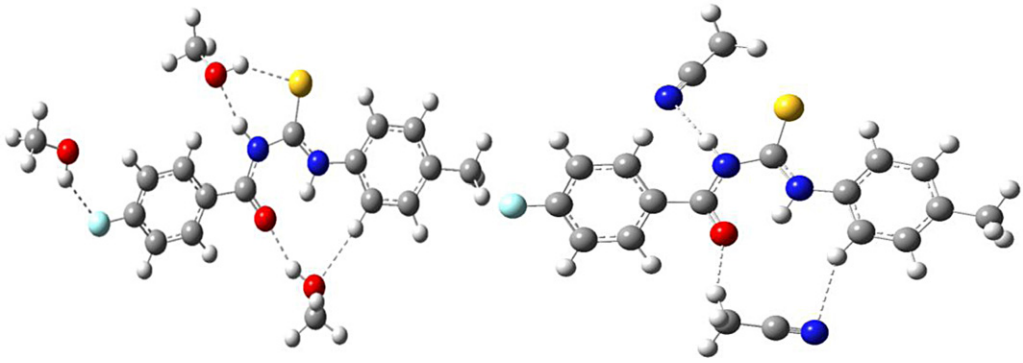

Fig. 3. Complexes of FBTT4 with methanol and acetonitrile molecules in the first solvation shell.

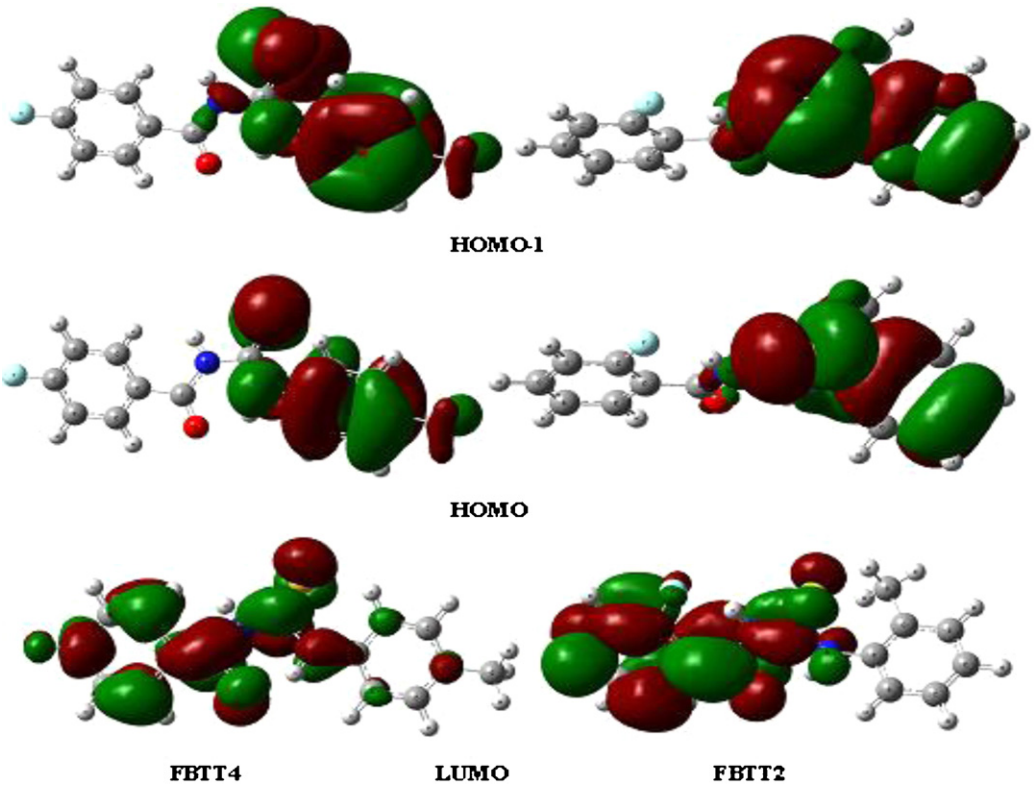

Fig. 4. Frontier molecular orbitals of both FBTTs.

interactions. As we know, in crystals, there are a number of intermolecular hydrogen bond interactions. In the solution of the concentration of 10^{-4} mol L^{-1}, the interactions should exist. Restricted by calculation resource, we have not further calculated the larger scale system considering the interactions between the solute molecules.

The calculated absorption curves of FBTT2 match well with experimental spectra in all solvents. We have not observed the unusual solvent effects in cyclohexane, dichloromethane and THF. Because of the formation of two intramolecular hydrogen bonds of FBTT2, the intermolecular hydrogen bond interactions in the crystal of FBTT2 are weaker than that in the FBTT4. The calculation ignoring the interactions between solute molecules in a dilute solution is not enough to bring out the error. In acetonitrile and methanol, the numbers of solvent molecules are also more than that of the solute molecules. Thus, the calculation which omit the interaction between the FBTT2 molecules and consider the intermolecular interactions between the solute and solvent molecules should be much more reasonable.

In a word, the intramolecular hydrogen bonds broaden the absorption band of $n \rightarrow \pi^*$ nature. And the intermolecular interactions between the solute and the solvent molecules cause the $\pi \rightarrow \pi^*$ absorption band to unusual blue shifts in the hydrogen bonding solvents. The increase of solvent polarity and the formation of intermolecular hydrogen bond interactions result in the decrease of absorption intensity.

3. Conclusion

Intramolecular hydrogen bonding interactions affect the intermolecular hydrogen bonding interactions. The different intermolecular hydrogen bonding interactions result in the different crystal packing of both isomers. The unusual blue shifts of the second absorption bands in polar solvents, acetonitrile and methanol, are due to the formation of intermolecular hydrogen bonds between FBTTs and solvent molecules. The intramolecular hydrogen bonds broaden the absorption band of the property of $\pi^* \rightarrow n$ transition. The TD-DFT/CPCM models adding the micro-solvent in the first shell obtain satisfactory results.

4. Experimental

Crystal structures were determined by X-ray diffraction with MERCURY CCD detector. The data were corrected for Lorentz and polarization effects. The structures were solved by direct methods [48] and expanded using Fourier techniques [49]. The absorption spectra have been determined in the solvents at 5×10^{-5} mol L^{-1}. The absorption spectra were recorded on a UV–VIS spectrophotometer, CARY50.

The ground-state minimum structures and their hydrogen-bonded complexes of both FBTTs are obtained by MP2 [50] method. The harmonic vibration frequency calculations confirm the stability of the structures. The absorption spectra are calculated by TD-DFT (B3LYP) for the first ten singlet states of the ground-state geometry. Solvent effects are considered by CPCM model [51–57] and the combinational CPCM model added the first solvent shell in hydrogen bond solvents [58,59]. Pople basis set, 6-31G (d) is used in all subsequent steps. All calculations have been performed with the Guassian 09 program package [60].

Appendix A. Supplementary data

Supplementary data associated with this article can be found, in the online version, at http://dx.doi.org/10.1016/j.jfluchem.2012.09.005.

References

[1] K.L. Han, G.J. Zhao, Hydrogen Bonding and Transfer in the Excited State, John Wiley & Sons Ltd., UK, 2010.
[2] M.H. Abraham, Chemical Society Reviews 22 (1993) 73–83.

[3] A.L. Sobolewski, W. Domcke, Journal of Physical Chemistry A 111 (2007) 11725–11735.
[4] Z.G. Lan, L.M. Frutos, A.L. Sobolewski, W. Domcke, Proceedings of the National Academy of Sciences 105 (2008) 12707–12712.
[5] C. Hao, R. Wang, M.X. Zhang, H. Yang, M.H. Ge, J.W. Chen, J.S. Qiu, Journal of Photochemistry and Photobiology A: Chemistry 217 (2011) 219–223.
[6] G.J. Kearley, F. Fillaux, M.H. Baron, S. Bennington, J. Tomkinson, Science 264 (1994) 1285–1289.
[7] H. Zhang, S.F. Wang, Q. Sun, S.C. Smith, Physical Chemistry Chemical Physics 11 (2009) 8422–8424.
[8] L. Serrano-Andres, M. Merchan, Journal of Photochemistry and Photobiology C: Photochemistry Review 10 (2009) 21–32.
[9] C.J. Fecko, J.D. Eaves, J.J. Loparo, A. Tokmakoff, P.L. Geissler, Science 301 (2003) 1698–1702.
[10] K.I. Priyadarsini, Journal of Photochemistry and Photobiology C: Photochemistry Review 10 (2009) 81–95.
[11] J.L.J. Blanco, P. Bootello, J.M. Benito, C.O. Mellet, J.M.G. Fernández, Journal of Organic Chemistry 14 (2006) 5136–5143.
[12] L. Nie, Z. Li, J. Han, X. Zhang, R. Yang, W.X. Liu, F.Y. Wu, J.W. Xie, Y.F. Zhao, Y.B. Jiang, Journal of Organic Chemistry 69 (2004) 6449–6454.
[13] F.Y. Wu, M.H. Hua, Y.M. Wua, X.F. Tana, Y.Q. Zhao, Z.J. Ji, Spectrochimica Acta Part A: Molecular and Biomolecular Spectroscopy 65 (2006) 633–637.
[14] R. Martínez-Máñez, F. Sancenón, Coordination Chemistry Reviews 250 (2006) 3081–3093.
[15] F.Y. Wu, L.H. Ma, Y.B. Jiang, Analytical Sciences (Supplement) 17 (2001) 801–803.
[16] F.Y. Wu, Z. Li, L. Guo, X. Wang, M.H. Lin, Y.F. Zhao, Y.B. Jiang, Organic & Biomolecular Chemistry 4 (2006) 624–630.
[17] H.B. Li, H.J. Yan, Journal of Physical Chemistry C 113 (2009) 7526–7530.
[18] P.D. Beer, P.A. Gale, Angewandte Chemie International Edition 40 (2001) 486–516.
[19] Y. Kubo, M. Tsukahara, S. Ishihara, S. Tokita, Chemical Communications 8 (2000) 653–654.
[20] L. Fabbrizzi, A. Leone, A. Taglietti, Angewandte Chemie International Edition 40 (2001) 3066–3069.
[21] F.Y. Wu, Y.B. Jiang, Chemical Physics Letters 355 (2002) 438–444.
[22] J.L. Wu, Y.B. He, Z.Y. Zeng, L.H. Wei, L.Z. Meng, T.X. Yang, Tetrahedron 60 (2004) 4309–4314.
[23] L. Rodríguez, S. Alves, J.C. Lima, A. Parola, F. Pina, C. Sorianoc, T. Albelda, E. García-España, Journal of Photochemistry and Photobiology A 159 (2003) 253–258.
[24] G. Hennrich, H. Sonnenschein, U. Resch-Genger, Tetrahedron Letters 42 (2001) 2805–2808.
[25] X.A. Zhang, W.D. Woggon, Journal of the American Chemical Society 127 (2005) 14138–14139.
[26] B.E. Smart, Journal of Fluorine Chemistry 109 (2001) 3–11.
[27] H.G. Bonacorso, A.P. Wentz, R.V. Lourega, C.A. Cechinel, T.S. Moraes, H.S. Coelho, N. Zanatta, M.A.P. Martins, M. Hoerner, S.H. Alves, Journal of Fluorine Chemistry 127 (2006) 1066–1072.
[28] M. Jagodzinska, F. Huguenot, G. Candiani, M. Zanda, ChemMedChem 4 (2009) 49–51.
[29] R. Filler, R. Saha, Future Medicinal Chemistry 1 (2009) 777–791.
[30] L. Hennig, K. Ayala-Leon, J. Angulo-Cornejo, R. Richter, L. Beyer, Journal of Fluorine Chemistry 130 (2009) 453–460.
[31] F.M.D. Ismail, Journal of Fluorine Chemistry 118 (2002) 27–33.
[32] Y. Yonetoku, H. Kubota, Y. Okamoto, J. Ishikawa, M. Takeuchi, M. Ohta, S. Tsukamoto, Bioorganic & Medicinal Chemistry 14 (2006) 5370–5383.
[33] D.J. Wang, L. Fan, C.Y. Zheng, Z.D. Fang, Journal of Fluorine Chemistry 131 (2010) 584–586.
[34] D.R. Salahub, M.C. Zerner, The Challenge of d and f Electrons, ACS, Washington, DC, 1989.
[35] C. Lee, W. Yang, R.G. Parr, Physical Review B 37 (1988) 785–789.
[36] B. Miehlich, A. Savin, H. Stoll, H. Preuss, Chemical Physics Letters 157 (1989) 200–206.
[37] W. Yang, W.Q. Zhou, Z.J. Zhang, Journal of Molecular Structure 828 (2007) 46–53.
[38] E.U.K. Gross, J.F. Dobson, M. Petersilka, Recent Advances in Density Functional Methods, vol. 1, World Scientific, Singapore, 1995.
[39] F. Furche, R. Ahlrichs, Journal of Chemical Physics 117 (2002) 7433–7447.
[40] G. Scalmani, M.J. Frisch, B. Mennucci, J. Tomasi, R. Cammi, V. Barone, Journal of Chemical Physics 124 (2006) 094107 (p1–p15).
[41] M. Cossi, V. Barone, Journal of Chemical Physics 115 (2001) 4708–4717.
[42] J. Tomasi, B. Mennucci, R. Cammi, Chemical Reviews 105 (2005) 2999–3094.
[43] A.K. Rappe, C.J. Casewit, K.S. Colwell, W.A. Goddard III, W.M. Skiff, Journal of the American Chemical Society 114 (1992) 10024–10035.
[44] I. Yavari, M. Bagheri, K. Porshamsian, S. Ali-Asgari, Journal of Sulfur Chemistry 28 (2007) 269–273.
[45] C.M. Sheldrick, T.R. Schneider, Methods in Enzymology 277 (1997) 319–343.
[46] L.J.J. Farrugia, Journal of Applied Crystallography (1997) 565.
[47] B. Valeur, Molecular Fluorescence: Principles and Applications, Wiley-VCH Verlag GmbH, Weinheim, Germany, 2001.
[48] A. Altomare, M.C. Burla, M. Camalli, G.L. Cascarano, C. Giacovazzo, A. Guagliardi, A.G.G. Moliterni, G. Polidori, R. Spagna, Journal of Applied Crystallography 32 (1999) 115–119.
[49] P.T. Beurskens, G. Admiraal, G. Beurskens, W.P. Bosman, R. de Gelder, R. Israel, J.M.M. Smits, The DIRFID-99 Program System, Technical Report of the Crystallography Laboratory, University of Nijmegen, Nijmegen, The Netherlands, 1999.
[50] A.E. Azhary, G. Rauhut, P. Pulay, H.J. Werner, Journal of Chemical Physics 108 (1998) 5185–5193.
[51] M.E. Casida, C. Jamorski, K.C. Casida, D.R. Salahub, Chemical Physics 108 (1998) 4439–4450.
[52] M. Cossi, N. Rega, G. Scalmani, V. Barone, Journal of Computational Chemistry 24 (2003) 669–681.
[53] S. Miertuša, E. Scroccob, J. Tomasi, Chemical Physics 55 (1981) 117–129.
[54] S. Miertu, J. Tomasi, Chemical Physics 65 (1982) 239–245.
[55] M. Cossia, V. Baronea, R. Cammib, J. Tomasic, Chemical Physics Letters 255 (1996) 327–335.
[56] V. Barone, M. Cossi, Journal of Physical Chemistry A 102 (1998) 1995–2001.
[57] J. Tomasi, B. Mennuccia, E. Cancès, Journal of Molecular Structure 464 (1999) 211–226.
[58] G.J. Zhao, K.L. Han, Physical Chemistry Chemical Physics 12 (2010) 8914–8918.
[59] K. Peng, W. Yang, W.Q. Zhou, International Journal of Quantum Chemistry 109 (2009) 811–818.
[60] M.J. Frisch, G.W. Trucks, H.B. Schlegel, G.E. Scuseria, M.A. Robb, J.R. Cheeseman, G. Scalmani, V. Barone, B. Mennucci, G.A. Petersson, H. Nakatsuji, M. Caricato, X. Li, H.P. Hratchian, A.F. Izmaylov, J. Bloino, G. Zheng, J.L. Sonnenberg, M. Hada, M. Ehara, K. Toyota, R. Fukuda, J. Hasegawa, M. Ishida, T. Nakajima, Y. Honda, O. Kitao, H. Nakai, T. Vreven, J.A. Montgomery Jr., J.E. Peralta, F. Ogliaro, M. Bearpark, J.J. Heyd, E. Brothers, K.N. Kudin, V.N. Staroverov, R. Obayashi, J. Normand, K. Raghavachari, A. Rendell, J.C. Burant, S.S. Iyengar, J. Tomasi, M. Cossi, N. Rega, J.M. Millam, M. Klene, J.E. Knox, J.B. Cross, V. Bakken, C. Adamo, J. Jaramillo, R. Gomperts, R.E. Stratmann, O. Yazyev, A.J. Austin, R. Cammi, C. Pomelli, J.W. Ochterski, R.L. Martin, K. Morokuma, V.G. Zakrzewski, G.A. Voth, P. Salvador, J.J. Dannenberg, S. Dapprich, A.D. Daniels, Ö. Farkas, J.B. Foresman, J.V. Ortiz, J. Cioslowski, D.J. Fox, Gaussian 09, Gaussian, Inc., Wallingford, CT, 2009.